Opto-Electronic Advances

Review

2019, Vol. 2, No. 1

DOI: 10.29026/oea.2019.180017

Laser machining of transparent brittle materials: from machining strategies to applications

Xiaozhu Xie[1,2]*, Caixia Zhou[1], Xin Wei[1], Wei Hu[1] and Qinglei Ren[1]

Transparent brittle materials such as glass and sapphire are widely concerned and applied in consumer electronics, optoelectronic devices, etc. due to their excellent physical and chemical stability and good transparency. Growing research attention has been paid to developing novel methods for high-precision and high-quality machining of transparent brittle materials in the past few decades. Among the various techniques, laser machining has been proved to be an effective and flexible way to process all kinds of transparent brittle materials. In this review, a series of laser machining methods, e.g. laser full cutting, laser scribing, laser stealth dicing, laser filament, laser induced backside dry etching (LIBDE), and laser induced backside wet etching (LIBWE) are summarized. Additionally, applications of these techniques in micromachining, drilling and cutting, and patterning are introduced in detail. Current challenges and future prospects in this field are also discussed.

Keywords: transparent brittle materials; glass; sapphire; laser machining

Xie X Z, Zhou C X, Wei X, Hu W, Ren Q L. Laser machining of transparent brittle materials: from machining strategies to applications. *Opto-Electronic Advances* **2**, 180017 (2019).

Introduction

Transparent brittle materials are highly important materials in applications to micro/nano-fabrication, microelectronic chips, biochips, biological channels, microfluidics, and optoelectronic devices because of its wide light transmission region, high corrosion resistance, chemical stability, high electrical insulation property, and high temperature and thermal shock resistance. For example, hard tempered glass is used as a display screen for smart phones. Hard and scratch-resistant sapphire can be applied to 3C products such as LED substrate, protection mirrors of mobile phone camera, and cover glass of smart watches, etc. Moreover, it is the preferred material of motion sensor, which is the important component of the autonomous driving technology, equipment for road monitoring and warning and display equipment of large window. It can protect the normal operation of equipment even in the harsh operating environment. At the same time, its material properties have been favored by military drones, deep sea dive equipment and aerospace technology.

Transparent brittle materials have superior performance and market applications, but hardness and brittleness are also intrinsic characteristics of them which can easily lead to cracking and chipping during machining of the material. Future trends of glass, sapphire and other materials in practical applications are becoming thinner and thinner, which lead to the higher requirements of machining quality. Therefore, the machining of ultra-precision cutting, drilling, grooving and surface structure on these brittle and fragile materials is currently a great challenge.

Traditional machining methods for transparent brittle materials mainly include diamond cutting[1] and chemical etching[2]. Cracks and pits are prone to generate during machining, and the machining size is poorly controlled. Moreover, machining precision and efficiency are low, so it is difficult to meet the machining requirements. Non-traditional methods include hot air-jet cutting[3], water-jet cutting[4], and laser machining. Among them laser machining has several advantages: (i) The machining method of "non-contact" is a powerful characteristic that avoids the negative effects of tool wear, breakage, and mechanical stress; (ii) The materials with high hardness and high melting point can be processed by this method,

[1]Laser Micro/Nano Processing Lab, School of Electromechanical Engineering, Guangdong University of Technology, Guangzhou 510006, China; [2]Department of Experimental Teaching, Guangdong University of Technology, Guangzhou 510006, China

*Correspondence: X Z Xie, E-mail: xiaozhuxie@gdut.edu.cn

Received 20 September 2018; accepted 7 January 2018; accepted article preview online 14 January 2018

and the machining quality and precision is high; (iii) It is easy to achieve automatically and intelligently, and the flexible machining is possible. The laser machining technology for transparent brittle materials is mainly divided into laser dry machining and laser wet machining[5]. Among them, the methods of laser dry machining include laser full cutting[6], laser scribing[7], laser stealth dicing[8], laser filament[9], and laser induced backside dry etching (LIBDE)[10]. Laser wet machining is mainly divided into laser induced front wet etching (LIFWE)[11] and laser induced backside wet etching (LIBWE)[12].

In this paper, the methods of laser machining transparent brittle materials are introduced, such as laser full cutting, laser scribing, laser stealth dicing, laser filament, LIBDE, and LIBWE. Comparing the advantages and disadvantages of several machining methods, the applications of laser machining transparent brittle materials in micromachining, drilling and cutting, and patterning are reviewed, and the opportunities and challenges of laser machining of transparent brittle materials are discussed.

Methods of laser machining transparent brittle materials

Laser dry machining

Laser full cutting

Laser full cutting, also known as laser cutting, refers to irradiate the workpiece by using a focused laser beam of high-energy density, which is achieved by melting, vaporizing, or generating thermal stress. Since glass and sapphire are dielectric materials, the absorption of laser photons by laser irradiation excites electrons in the material, causing electrons to transit from a steady state to some excited state. When a long pulse laser acts on it, the material absorbs a single photon. When the energy exceeds the band gap of the material, the excited electrons transition is from the valence band to the conduction band. Ultrafast lasers can achieve electronic valence-to-conduction band transitions with multi-photon absorption due to their extremely high peak power density, even if the single photon energy is lower than the band gap of material. Laser cutting of glass and sapphire has two machining methods: one is full cutting (similar to the way of cutting sheet metal, using a cutting head) and the other is layer-by-layer scanning (using a galvanometer).

Sapphire and glass belong to the material of wide-band gap dielectric, and there is not a large amount of electrons in itself. When the long pulse laser acts on it, it corresponds to the thermal ablation process. Melting, vaporization, recast layer, surface micro cracks, thermal stress and fracture are caused, which limits the improvement of machining quality, as shown in Fig. 1(a). At the same time, the application range of nanosecond laser machining of transparent brittle materials such as sapphire and glass is different. For example, sapphire can be processed by infrared, green, and ultraviolet (wavelength of 1064/532/355 nm) nanosecond lasers, but glass can't be processed by 1064 nm near-infrared laser. However, glass can be processed with mid-infrared (wavelength of 10640 nm), green and ultraviolet (wavelength of 532/355 nm) lasers.

Researchers[13–14] pointed out that the pulse duration is most favorable for fine micromachining on the picosecond scale, and the pulse width of around 10 ps is better for laser micromachining. When an ultrashort pulse laser acts on a transparent medium, free electrons will be generated. Meanwhile, the generation of carriers must be completed by multi-photon ionization, tunneling effect or avalanche ionization, which is also the three typical ionization processes of femtosecond laser acting on transparent medium[15]. Multi-photon ionization occurs when the laser pulse electric field is regarded as perturbation. If the laser electric field is sufficiently high, the band will be severely distorted, resulting in the occurrence of tunneling ionization. When electrons at higher energy levels return to the bottom of the conduction band by in-band transitions, the electron in the valence band is simultaneously excited to the conduction band, resulting in avalanche ionization. Since the high peak power can generate strong nonlinear effects inside the transparent medium, the short pulse width can effectively suppress the for-

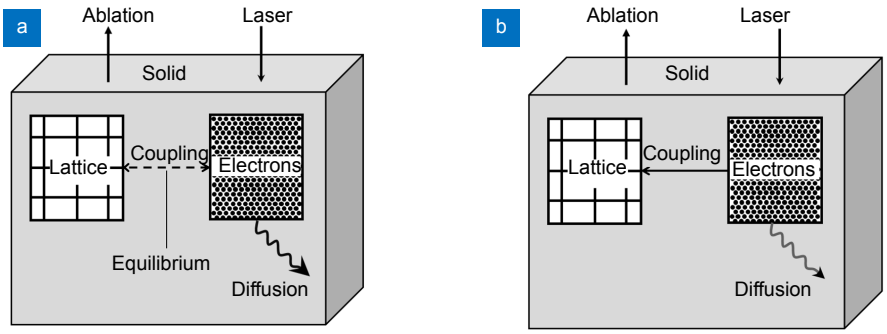

Fig. 1 | Mechanism of laser direct machining transparent brittle materials with long-pulse and ultrashort pulse. (**a**) Schematic diagram of long-pulse laser action. (**b**) Schematic diagram of ultrashort pulse laser. Figure reprinted with permission from ref.[16], Springer-Verlag.

mation of the heat affected zone. Therefore, ultra-short pulse machining of transparent brittle materials can achieve high-precision "cold machining" without obvious thermal stress and micro-cracks. It greatly improves the machining quality, which is shown in Fig. 1(b).

Laser scribing

Laser scribing for brittle materials was originally proposed by Garibotti[7]. It is a two-stage process, as shown in Fig. 2. In the first stage, the laser beam is focused on the focal plane of the workpiece, and a groove or deep hole with a depth of one third to one half of the material thickness is generated by the laser (Fig. 2(a)). In the second stage, breaking by applying a mechanical force takes place normally with the help of vacuum chucks or by mechanical force[17] (Fig. 2(b)). At the same time, the breaking can also be applied by spraying water, jet, or laser beam to apply thermal stress or laser-induced thermal shock[18–19].

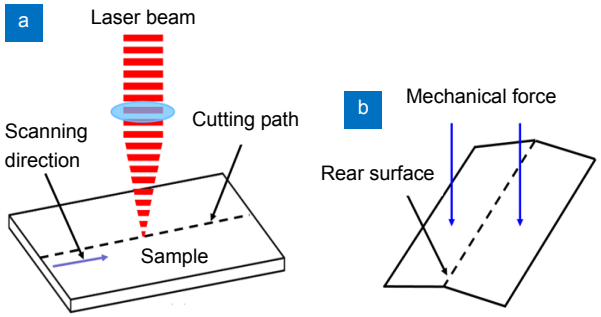

Fig. 2 | Laser scribing and breaking. (**a**) Laser scribing. (**b**) Mechanical breaking. Figure reprinted with permission from ref.[17], Springer-Verlag.

The general processing method is laser direct scanning. But Hong and co-workers[20] have put forward a new method of pocket scanning, which in computer assisted manufacturing (CAM) is defined as the "parallel overlapped scanning of paths". The results showed that the number of microcracks formed around the ablated grooves in pocket scanning was reduced significantly compared with that produced in laser direct scanning. For the purpose of theoretically clarifying the laser cross scribe mechanism, the laser cross scribe experiment and the three dimensional thermal elasticity analysis by means of the FEM were performed and the progress of the second scribing in the laser cross scribe was discussed by Yamamoto et al.[21].

The common laser scribing is focused on the front surface. However, Ahmed and co-workers[17] proposed an idea of fast cutting a display glass plate where the sample is pre-processed micromachining single shot rear-surface and internal void arrays aligned on working plane prior to glass cleaving. The results showed that the double-line void array scheme is more reliable than the single-line void array scheme.

Laser stealth dicing

In recent years, a laser dicing technique called stealth dicing has been introduced. First, a laser beam of a translucent wavelength is focused inside a brittle material and scanned along a predetermined path to form a starting point for division inside the brittle material, and a stress layer is formed, and then an external force is applied to the brittle material to separate it. Figs. 3(a) and 3(b) show the basic principle of the stealth dicing. When the laser is focused on the inside of the wafer, the crystal near the focusing is locally melted. When the temperature near the melting zone cools below the melting point of the material, cracks are generated in the recrystallized portion of the wafer. Then the wafer is broken by applying tensile stress in the vertical direction by tape expansion. The technology was originally applied to laser cutting of semiconductor wafers, and subsequently applied to the cutting of materials such as glass and sapphire.

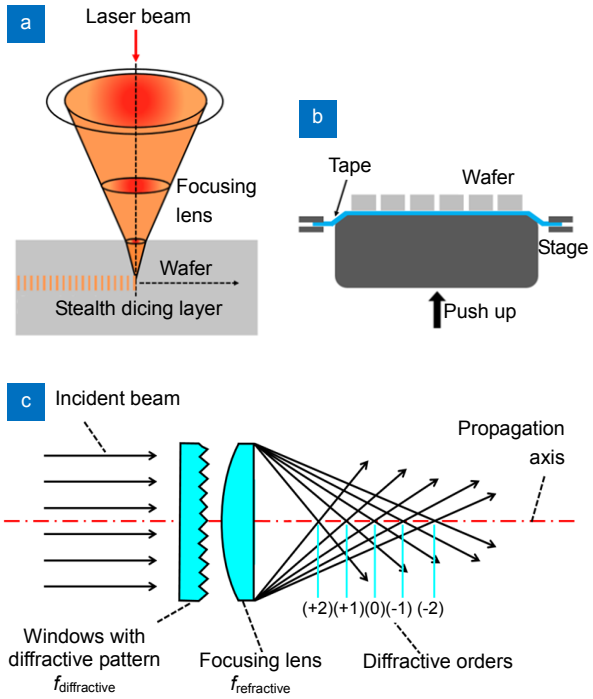

Fig. 3 | Representation of laser stealth dicing sapphire wafer. (**a**) Schematic illustration of the process for slicing. A laser beam is focused on point inside the wafer to form a stealth dicing (SD) layer. (**b**) The separation process. Fixing the expanded film with the wafer adhered to the wafer on a two-dimensional platform, and the sapphire wafer is separated by applying an external force. (**c**) Commonly used multifocal optical system diagram. Figure reproduced from: (a), (b) ref.[22], Chinese Journal of Lasers; (c) ref.[23].

Single-focus laser processing is difficult to ensure the quality of brittle materials along the thickness direction, and its taper is difficult to control. Therefore, in order to improve processing efficiency and processing quality, many researchers[23-26] have explored and studied laser multifocal processing. The implementation of multifocal system functions usually requires the combination of diffractive optical elements and focusing lenses, mainly for

the cutting of transparent materials. The spacing and number of focusing can be adjusted and controlled. The realization of the function of multifocal optical system usually requires the combination of Fresnel diffraction shaping lens and focusing lens (Fig. 3(c)). Fresnel lens has the characteristics of spotlight. Each circular groove can realize the function of focusing lens, and the light emitted from the same circular groove will focus together to form the center focus. But the laser beams emitted from different grooves are focused on different positions in the same horizontal direction, and eventually forming different focusing. The space between the focusing can be varied by adjusting another focusing lens. Several techniques for laser cutting glass based on stealth dicing were reported in some literatures[27–28]. For example, stealth dicing can be achieved using dual spot optics[29–30], or multi-pass dotted line[17, 31].

Laser filament

When the incident power of the laser exceeds the critical power (3 GW in air), the propagating beam does not show significant divergence due to the combined effects of various optical effects[32]. And a stable self-guided transmission is formed while maintaining stable energy transmission. It maintains long-distance transmission in an almost constant size, and its transmission length is at least several times longer than the Rayleigh length[33–34], forming a typical nonlinear phenomenon of the ultrafast laser in the medium-laser filament. Researchers have proposed self-guided model[35], moving focus model[36] and dynamic spatial compensation model[37] to explain the main characteristics of the phenomenon of filamentation. The basic physical mechanism of the filamentation is widely accepted as the dynamic balance between the self-focusing of the laser beam caused by the optical Kerr effect and the plasma defocusing effect caused by weak ionization[38]. The length of the filament depends on the peak power of the incident laser and the loss of photons derived from multi-photon ionization and plasma inverse bremsstrahlung during transmission.

Gaussian beams are the most common beam shape for material machining, but it is not feasible for the requirements of a given material configurations or applications. For example, Song et al.[39] theoretically has studied Bessel, Gaussian, and Laguerre modes of femtosecond filamentation. They find that the lengths of the filament and the plasma channel induced by the Bessel incident beam is much longer than the other transverse modes with the same peak intensity, pulse duration, and beam diameter. Laser filament is a nonlinear optical phenomenon, which is the transmission of ultrafast laser in transparent media. The material is cut based on a "focus extended" filament. The Bessel beam has several intrinsic properties: (i) The intensity profile is more uniform along the propagation compared to a Gaussian beam; (ii) The beam presents a good stability under nonlinear propagation in dielectric materials; (iii) The beam has the self-reconstruction properties[40].

Laser induced backside dry etching (LIBDE)

LIBDE uses solid layers (metal or non-metal materials) as absorbers. The technology was studied by many researchers[41–43]. There are two main processing methods, one is that there is a gap distance between the absorber and the target[44], and the other is that the absorber is direct contact with the target for processing[45]. Pan and co-workers[46] studied the fabrication of micro-texture channel on glass by laser-induced plasma-assisted ablation. There is a certain gap distance between glass workpiece and sacrificial material. First, several phenomena appear on the upper surface of sacrificial material, such as heating, melting, vaporization and the formation of plasma. Then the glass workpiece is heated, melted and vapored by hot plasma. Finally, the molten glass material is removed and micro-channel forms on the glass surface. Gao and co-workers[47] show that the expansion of plasma also generates a shock wave during processing which induces a formidable recoil pressure upon the melt pool of glass. The molten glass material is removed by this shock wave and micro-channel forms on the glass surface. A method for generating a very smooth three-dimensional crystalline metal nanoscale structure has been developed. And large, uniform nanopatterns with an aspect ratio of five were successfully produced.

Moreover, Chao and co-workers[48] explored a relatively novel laser induced dry etching technique which was based on using a nonmetallic target to etch solar glass and interpreted the etching mechanism by using a ceramic wafer as an absorber. Initially, there is no gap distance between the glass and the ceramic wafer. After the laser action, a gap is formed between the solar glass and the wafer; the heat conductivity will be reduced and eventually blocked by the air gap. Then the etching process will cease. It is shown that Al_2O_3 particles mainly play the role of energy conversion and heat conduction during the etching process.

Researchers[45,49] also used LIBDE for laser patterning. The authors' group and co-workers[50] used graphite as the absorber for laser patterning on glass, and the glass substrate was in close contact with the graphite plate pressed by external force. In the first stage, the graphite target was ablated by pulsed laser irradiation (Fig. 4(a)), graphite particles vaporized immediately and created a dense plasma plume. In the second stage, the plasma exploded violently in the limited space and continued absorbing the laser energy as the laser pulse was applied. The third stage was the rapid quenching of the high temperature high-pressure plasma (Fig. 4(b)). Under the effect of local high temperature and high pressure, the graphite particles were separated from the graphite surface quickly, contacted with the melting glass surface, and finally combined with the surface of the glass, forming a black pattern (Figs. 4(c) and 4(d)). A black laser pattern realized on a glass substrate is shown in Fig. 4(e).

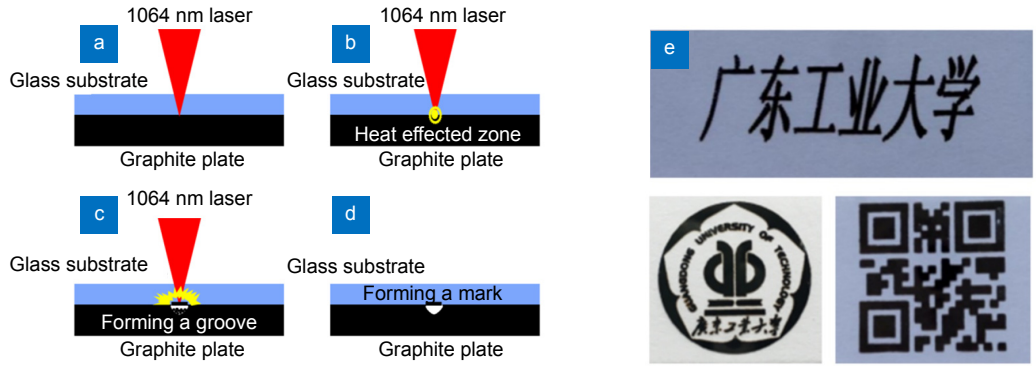

Fig. 4 | (**a**–**d**) The physical process of black color laser patterning of glass substrates. (**e**) Black laser pattern of glass substrate. Figure reproduced from: (a)–(d) ref.[50], Optical Society of America.

Laser wet machining

Laser wet machining includes laser front wet machining and laser induced backside wet etching (LIBWE). It has unique advantages in machining the materials of heat sensitive, high hard and brittle, and high precision requirements. However, the working liquid of the laser front wet etching is placed on the workpiece. Then the liquid has a large loss of the laser reflection, the light absorption and scattering in the liquid is large. Therefore, the droplet on the workpiece acts as a lens to concentrate the beam so that the focus is not easily controlled. Then the beam quality is degraded and the surface quality is poor. Relatively, the focus of LIBWE is easier to control, the machining quality and precision are high, and the damage is small. Therefore, only the theoretical model of laser induced backside wet etching transparent brittle materials is introduced.

Laser induced backside wet etching (LIBWE)

LIBWE refers to the technique of applying working liquid on the surface of workpiece and then focusing the beam on the liquid-solid interface for machining. The technology is the main research method for machining the microstructure of transparent brittle materials. In this way, the microstructure can be prepared in transparent materials such as quartz glass or sapphire more quickly and accurately. The working solutions used in LIBWE are mainly organic solutions, metal salt solutions and mixed solutions containing metal particles, and have a direct influence on the removal model and mechanism.

(a) Removal mechanism and model

In recent years, many researchers[51–53] have studied the removal model of LIBWE. Vass[54] established a one-dimensional thermal flow model by considering the phase transition of liquid and fused silica. Zimmer and co-workers[55–56] established a two-dimensional thermal flow model. The model considers the laser absorption in only one material as well as at the interface. The temperatures across the interface calculated analytically and numerically with constant coefficients (values at T_0 are used) are compared with the temperatures achieved with temperature dependent material properties. The analytically calculated temperatures agree with the numerical ones very well.

A three-dimensional thermal model was established by the authors' research group[57–58] to simulate the material removal during the LIBWE process by considering the material data variations of temperature, enthalpy change and latent heat fusion. The results indicated that the material removal of LIBWE was based on laser interaction with multilayer materials (sapphire substrate–deposition layer–liquid solution), as shown in Fig. 5(a). The pulse laser acted on the multi-media model, which was a repeated process in which the material was rapidly heated and then cooled until the next pulse was heated during

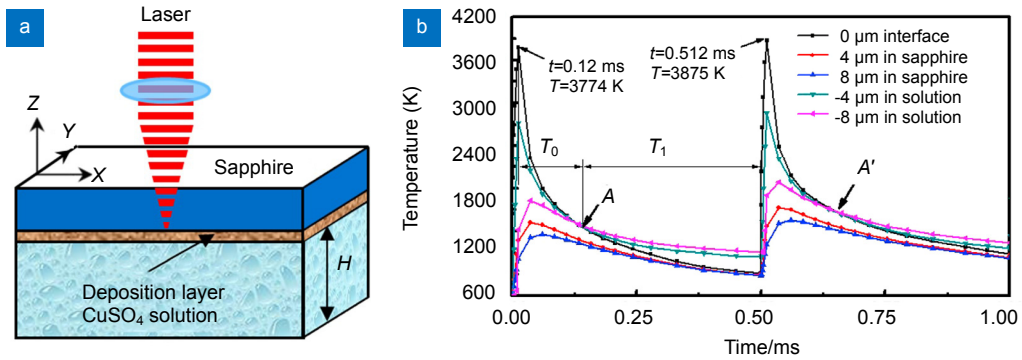

Fig. 5 | (**a**) Schematic diagram of three-dimensional model. (**b**) Temperature variation of different *Z* positions. Figure reprinted with permission from ref.[57], Elsevier Ltd.

the pulse width of each pulse, as shown in Fig. 5(b).

Furthermore, many researchers explained the removal mechanism of LIBWE by using these models. Sato et al.[59] showed that in laser-induced backside wet etching (LIBWE), the photo-activated region generated within organic solution would act on the glass surface and results in etching. It was indicated that the photo-activated region generated at the bottom of the trenches acted not only on the bottom of the trench but also on the sidewalls. Mitsuishi[60] showed that the machining was realized through material removal after melting by heat transfer from the absorbent particles. Hong and co-workers[61] revealed that the etching mechanism was a two-step process. The proposed mechanism of glass etching by the laser irradiation of 1064 nm to the copper sulphate solution is illustrated in Fig. 6.

(b) Cavitation and micro-jet

At the same time, many researchers find that the effect of cavitation and micro-jets on the etching mechanism is great. The dynamics process of cavitation bubble near a solid boundary was captured by Yang et al.[62]. It can be observed that a micro-jet directed to the wall surface is formed when the bubble collapses. In the process of LIBWE, the micro-jet impacts the molten material and takes away the debris generated during the etching process to achieve material removal[63].

The authors' group and co-workers[64–66] conducted experimental and theoretical studies on the cavitation phenomenon of LIBWE. Theoretical simulation of the dynamic of cavitation is shown in Fig. 7(a). As can be seen from the figure, the cavitation bubble has experienced two stages of expansion and collapse. And the cavitation bubble volume expands to the maximum at 45 μs. At this time the diameter of the cavitation bubble along the laser incident direction is 0.52 mm, and the whole period of the cavitation is 120 μs. In order to verify the correctness of the theoretical model, the dynamic process of cavitation is taken by high-speed camera, as shown in Fig. 7(b). It is found that the simulation results are basically consistent with the experimental results by comparing and analyzing the dynamic characteristics of the cavitation.

Furthermore, they[67] studied the effects of the laser repetition rate on the etching rate of sapphire using LIBWE with a 1064-nm ns laser and found that the etching rate was much higher when the laser was pulsed with a high repetition rate. By observing the evolution of laser-induced cavitation bubbles, they identified two etching mechanisms during LIBWE when high-repetition-rate laser pulses were used and determined that the incubation effect drove the transformation between the two mechanisms. The mechanism of the LIBWE process using near-infrared laser pulses with a low repetition rate and a high repetition rate is shown in Fig. 8.

Kim[68] showed that the dynamic characteristics of the cavitation bubble, chamber size, and other environments had a great impact on the etching mechanism. The study

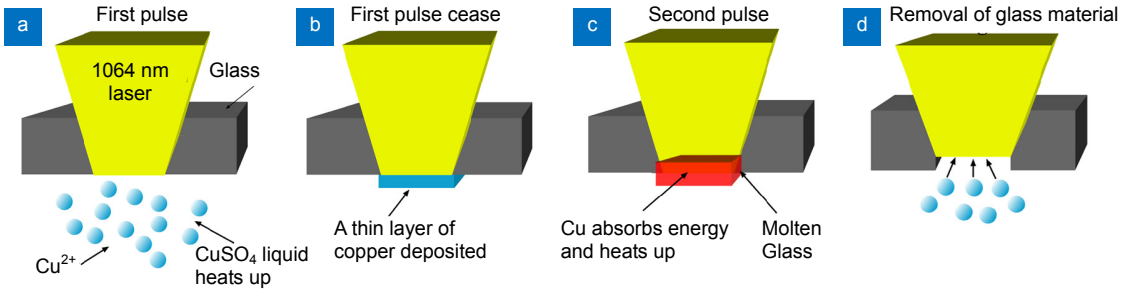

Fig. 6 | Proposed mechanism of the glass cutting using 1064 nm laser irradiation. (**a**) Laser irradiates from the top. (**b**) Copper deposition on the underneath of the glass. (**c**) The deposited copper absorbs the laser energy and heats up the immediate glass region. (**d**) Removal of the molten glass. Figure reprinted with permission from ref.[61], Springer-Verlag.

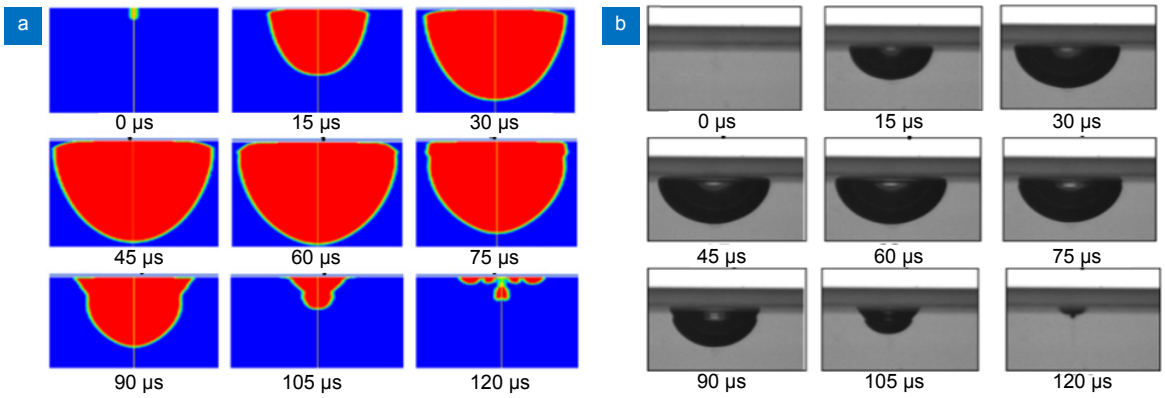

Fig. 7 | (a) Contours of the vapor volume fraction by simulation. **(b)** High-speed photography of cavitation bubble. Figure reproduced from ref.[64].

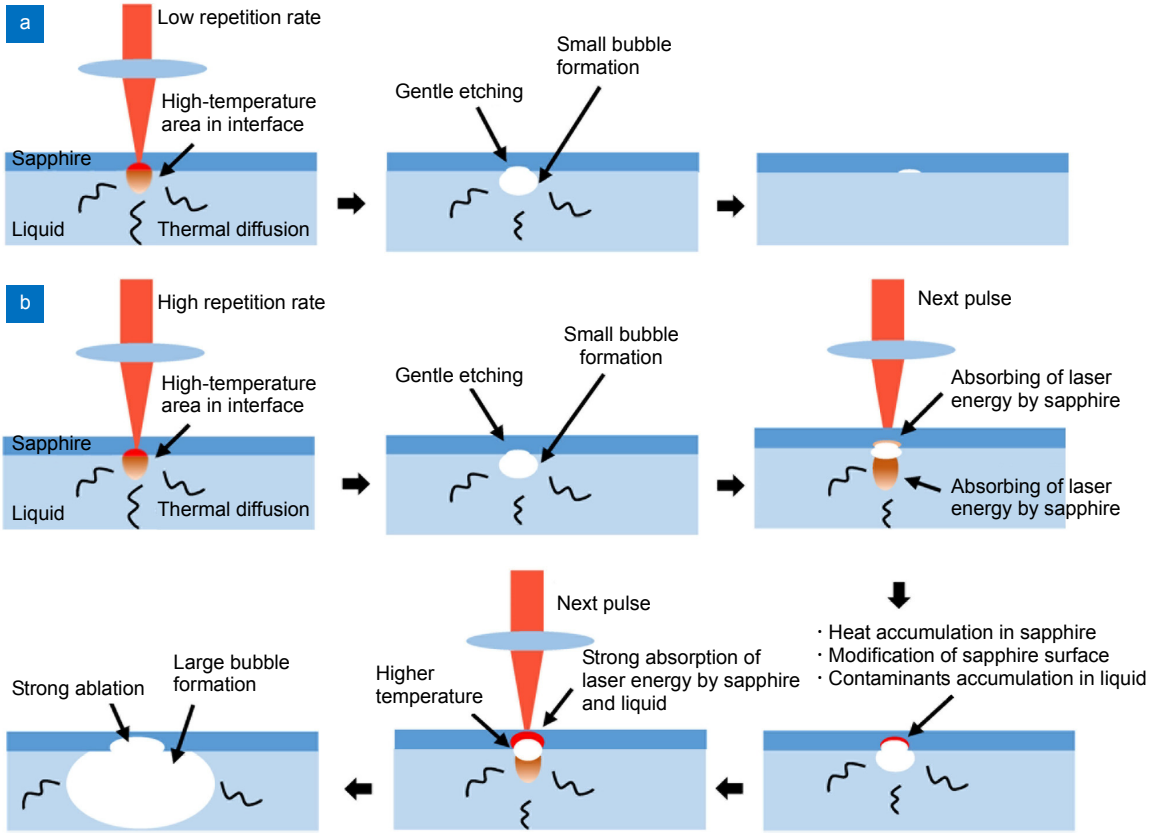

Fig. 8 | Schematic illustration of the LIBWE process using near-infrared laser pulses with (a) a low repetition rate and (b) a high repetition rate. Figure reprinted with permission from ref.[67], Elsevier Ltd.

confirmed that the photomechanical effects from the laser-induced bubble played a key role in the LIBWE process, revealing a linear relationship between the etch rate and the applied recoil momentum.

(c) Temperature and pressure

The temperature and pressure are also important factors affecting the mechanism of LIBWE. Liu and co-workers[69] studied the effect of liquid temperature on the collapse of cavitation bubble near a rigid boundary. The mechanism of liquid temperature influence on cavitation erosion also had been discussed. The results showed that liquid-jet impact pressure increases with liquid temperature and reached a peak, followed by a decrease. Through theoretical and experimental studies, Soliman et al.[70] found that the pressure and temperature during the process of LIBWE had a great influence on the machining quality. In addition, they estimated the pressure and the temperature inside the cavitation bubble on the basis of the agreement about the temporal variation of the size of the cavitation bubble.

The authors' research group[71–72] conducted an experimental study on the pressure detection during the process of LIBWE. The acquisition devices of pressure signals are shown in Fig. 9(a). The pressure signals are acquired at a laser energy density of 90.94 J/cm^2, pulse width of 100 ns, laser repetition frequency of 2.5 kHz, detection distance of 2 mm. When the laser repetition frequency is 2.5 kHz, the interval between adjacent laser pulses is 400 μs. The researches show that at least a plasma shock pressure signal and a pressure signal generated by a bubble collapse are generated during a period of 400 μs, and both pressure signals are generated by a laser pulse. Figures 9(b)–9(c) show the pressure signals during LIBWE at a laser repetition frequency of 2.5 kHz. The whole acquisition time of the pulse pressure signals is 108 ms (Fig. 9(b)). By amplifying part of the pressure signals, it can be found that the time interval between the pulse pressure signals a-c, c-e and e-g is 400 μs (Fig. 9(c)). This is in complete agreement with the corresponding pulse time interval corresponding to the laser repetition frequency of 2.5 kHz, that is, the pulse signals a, c, e and g are respectively generated by different laser pulses. The results show that the pulse pressure signals of a, c, e and g are generated by plasma shock waves. However, the pressure signals of b, d, f, and h are generated by the collapse of the bubble, that is, the time corresponding to the first collapse of the bubble.

In summary, the above-mentioned methods for laser machining transparent brittle materials have their own characteristics in terms of edge breakage, thermal stress, machining efficiency, machining quality, precision, system stability, process stability and cost. Table 1 compares the advantages and disadvantages of these machining methods.

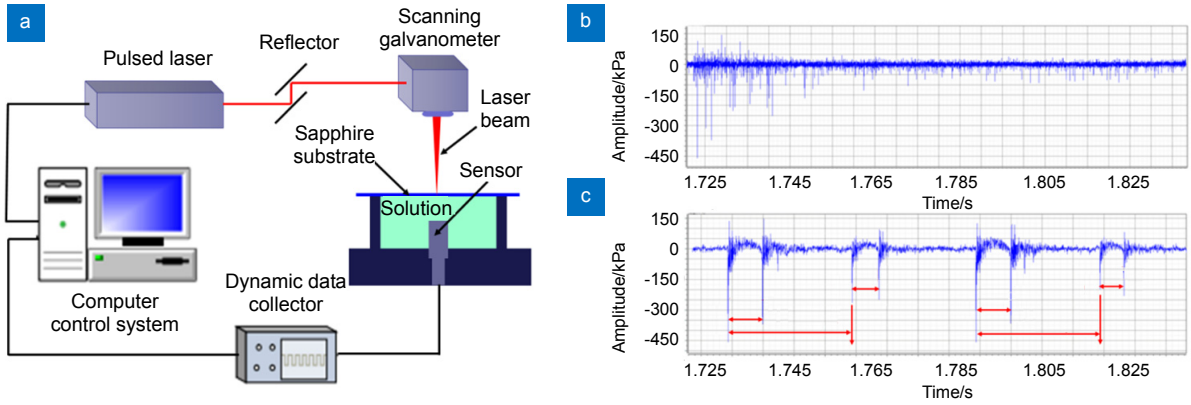

Fig. 9 | (**a**) Experimental device for acquiring pressure signals. (**b**) The whole acquisition time of the pulse pressure signals. (**c**) The part of the pressure signals under single-pulse. Laser energy density of 90.94 J/cm^2, solution concentration of 1 mol/L, pulse width of 100 ns, detection distance of 2 mm, laser repetition frequency of 2.5 kHz. Figure reproduced from ref.[72].

Table 1 | Comparison of various laser machining methods for transparent brittle materials.

	Nanosecond laser cutting	Ultrashort pulse laser cutting	Laser scribing	Laser stealth dicing	Laser filament	LIBDE	LIBWE
Edge breakage	Bigger	Smaller	Big	Small	Smaller	Medium	Smaller
Thermal stress	Bigger	Smaller	Big	Small	Smaller	Medium	Smaller
Machining efficiency	Higher	Lower	High	High	Lower	Low	Medium
Machining quality	Lower	Higher	Medium	High	Higher	Low	High
Process stability	Higher	Higher	Higher	High	High	Low	Low
Cost	Medium	High	Medium	High	Higher	Low	Lower

Applications

Micromachining

The applications of fabricating microstructures by laser on transparent materials are becoming wider and wider. And the machining requirements become higher and higher with the decreasing feature size and increasingly complex structure. Qiao et al.[73] reported the integration of microlens and microfluidic channels in fused silica glass chip using femtosecond laser micromachining. In addition, they demonstrated that the fabricated microlens exhibits good imaging performance with a 5× magnification, showing great potential in future lab-on-a-chip applications (Fig. 10).

Liu and co-workers[74] reported a technology of fabrication and stitching of internal 2D, 1D and multi-layer micro-gratings in fused silica glass using amplified Ti: sapphire femtosecond laser. Single-layer 1D (Fig. 11(a)) and 2D (Fig. 11(b)) as well as double-layer and stitched double-layer 1D (Figs. 11(c)–11(d)) internal micro-gratings with the size of 400 μm× 400 μm were fabricated using a femtosecond laser-based writing process and were characterized regarding their structure and properties. The double-layer gratings have a diffraction efficiency of about 25%, which is three times higher than that of single-layer counterparts. The stitched double-layer gratings have the doubled line density, which is not limited by optical diffraction limit. This multi-layer writing technique, combined with the 3D stitching technique, not only provides the high performance gratings, but also

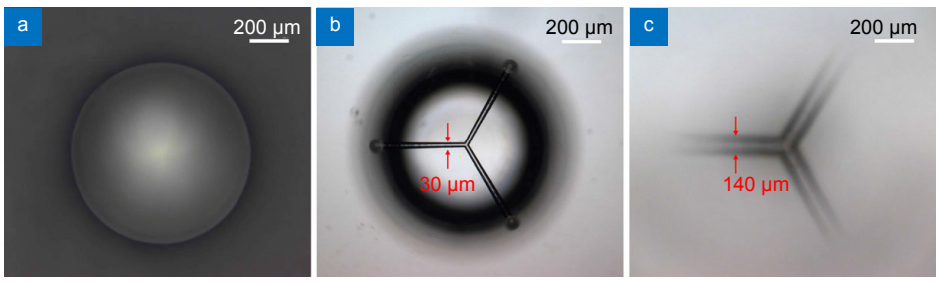

Fig. 10 | Optical micrograph. (**a**) Microlens. (**b**) Y-shaped microfluidic channel. (**c**) The enlarged image of the channel formed by the microlens. Figure reprinted with permission from ref.[73], Springer-Verlag.

opens the door to easily manipulate the diffraction efficiency of gratings through adjusting the inter-layer displacement and the line density by stitching the pitch.

Queste and co-workers[75] have manufactured micro-channels with a roughness of 100–150 nm in borosilicate glass by femtosecond laser. Fig. 12 shows details of the microfluidic chip. The strategy is to write lines spaced by 5 μm along the largest dimension. The channel was written first, then the reservoir, which causes the pitting in the overlapping zone which can be seen in Fig. 12(a). The profile angle is comprised between 80° and 85°. The surface is smooth around the machined areas. The bottom roughness is a bit high, on the order of 100–150 nm (Ra) (Fig. 12(d)).

Drilling and cutting

The fundamental properties of the picosecond laser machining of quartz glass were investigated by Ji et al.[76]. Circle and triangle micro-through-hole arrays without cracks, chips, and debris were machined in 0.3-mm-thick quartz glass by picosecond laser in air ambient. The diameter of each circle through-hole was 550 μm, and the side length of each triangle hole is 500 μm. 30 μm spacing between the adjacent hole edges and the smooth machined surface with *Ra*=0.8 μm roughness depicted the high precision of the high-density micro-through-hole arrays. The SEM micrograph of a circle micro-through-hole array is shown in Fig. 13.

Gao and Jiang[77–78] configured a copper sulfate mixed solution with high absorption rate for infrared laser. The sapphire is cut by LIBWE with the mixed solution. The surface quality of the cutting is good, and there is no obvious recast layer and chipping, as shown in Figs. 14(a)–14(b).

The tempered glass, quartz glass and solar glass were cut with a 532 nm nanosecond laser by Shen and co-workers[79]. The finished product was used as screen protectors for mobile phones, mobile phone panels, and solar panels. The samples are shown in Figs. 14(c)–14(e).

Patterning

Laser patterning is currently used for different purposes, such as bar codes for product tracking, brand logos or just decoration. Many researchers[80–82] have analyzed the

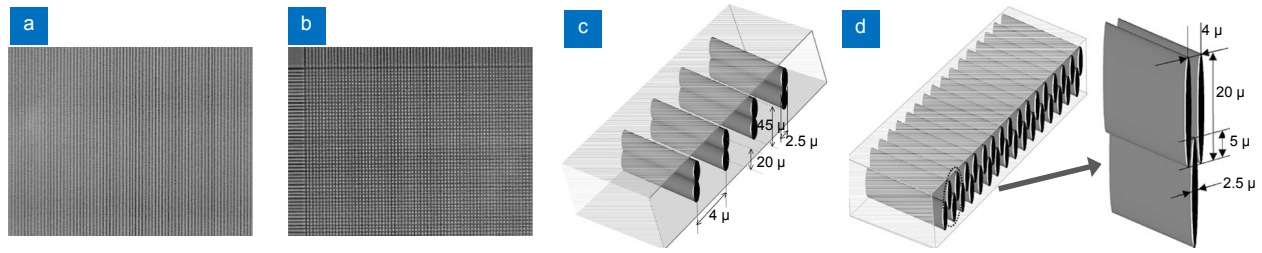

Fig. 11 | (**a**) Internal diffraction 1D micro-grating fabricated with fs laser. (**b**) Internal diffraction 2D micro-grating fabricated with fs laser. Schemes for (**c**) a double-layer 1D micro-grating, and (**d**) a stitched double-layer grating. Figure reprinted with permission from ref.[74], Springer-Verlag.

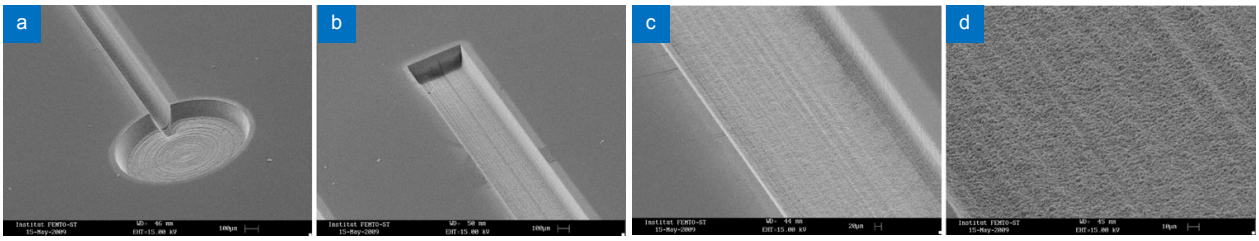

Fig. 12 | SEM images of details microchannels with reservoir ablated in borosilicate glass. (**a**) Channel with reservoir. (**b**) Channel. (**c**) Close-up of the channel. (**d**) Close-up of the bottom of the channel (Ra 100–150 nm). Figure reprinted with permission from ref.[75], Springer-Verlag.

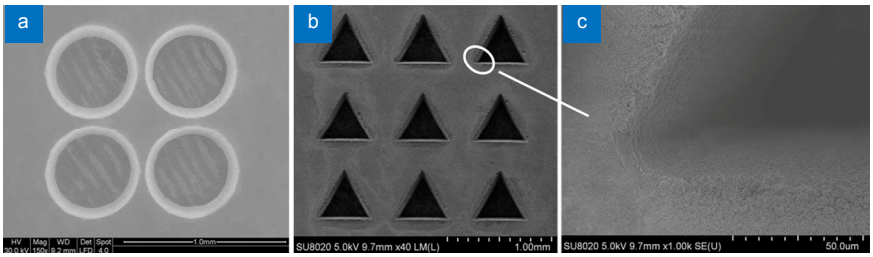

Fig. 13 | SEM micrograph. (**a**) Circle micro-through-hole array. (**b**) Triangle micro-through-hole array. (**c**) Enlarged image of tip angle of the triangle micro-hrough-hole. Figure reprinted with permission from ref.[76], Springer-Verlag, Berlin Heidelberg.

influencing factors of laser patterning. And they have been studying how to get good surface quality and durability of patterning. Zhang and co-workers[83] introduced the advantages of laser patterning technology and the difficulty of patterning glass surface. Patterning texts on glass with three different ways, and the effects of different parameters on each patterning method were investigated.

Sato and co-workers[84] fabricated micropit array structures on silica glass by fast beam scanning LIBWE , which was employed for fast and flexible laser patterning of glass materials. It was confirmed that micropits with maximum depths up to 0.35 μm could be fabricated by single pulse irradiation without crack formation.

Niino and co-workers[85–89] fabricated patterns using laser-induced backside wet etching (LIBWE). Well defined line-and-space and grid micropatterns, free of debris and microcracks, were obtained. A SEM micrograph of the line-and-space pattern on the surface of the fused silica sample is shown in Fig. 15a. The profile of the etched surface clearly demonstrates that the etched edge was quite sharp, and the bottom of the holes was very flat (Fig. 15(b)).

Sohn et al.[90] demonstrated the design and development of a synchronized femtosecond laser pulse switching system and its applications in nano-patterning of transparent materials. Using the synchronized laser system, they patterned synchronized nano-holes on the surface of and inside various transparent materials including fused silica glass and polymethyl methacrylate to replicate any image or pattern on the surface of or inside (transparent) materials. The surface of flint glass of type F2 is patterned with nanosecond KrF excimer laser ablation by Ihlemann et al.[91] The SEM images of crossed grating patterns on F2 glass is shown in Fig. 16.

Conclusions and outlook

We have summarized the theoretical model in the field of transparent brittle materials from the perspective of laser fabrication strategies and their wide applications. And the advantages and disadvantages of various methods are summarized. Finally, the applications in micromachining, drilling and cutting, and patterning are reviewed in detail.

With the widespread use of transparent brittle materials in products such as smartphones, LEDs, tablets, wearable devices, and touch screen displays, there are more and more lasers, laser systems, and related scientific

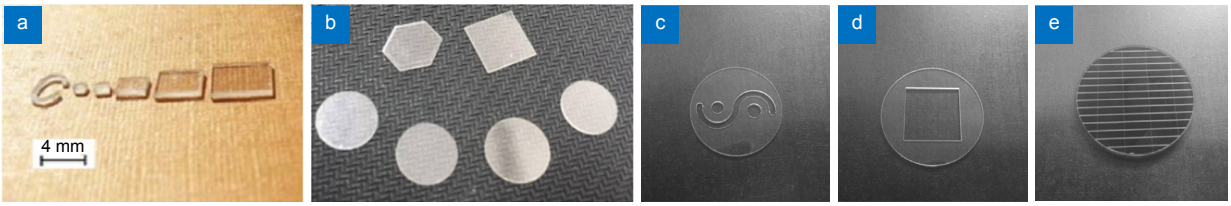

Fig. 14 | (**a**,**b**) Shaped cutting parts of sapphire cutting samples. (**c**) Tempered glass. (**d**) Quartz glass. (**e**) Solar glass. Figure reproduced with permission from: (a,b) ref.[77,78]. (c–e) ref.[79], Applied Laser.

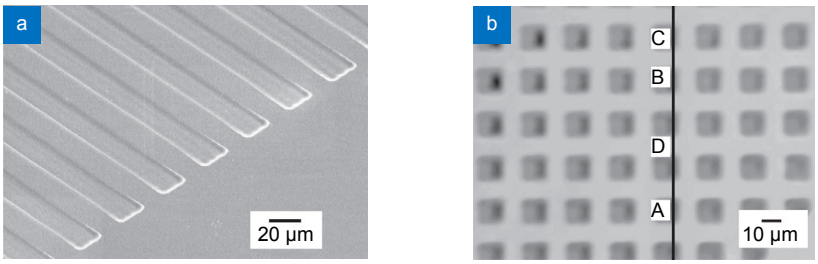

Fig. 15 | (**a**) SEM micrograph of the line-and-space pattern on fused silica observed at an inclined angle of 45°. (**b**) Confocal scanning laser microscopic picture of a grid pattern on fused silica. Figure reprinted with permission from ref.[85], Springer-Verlag.

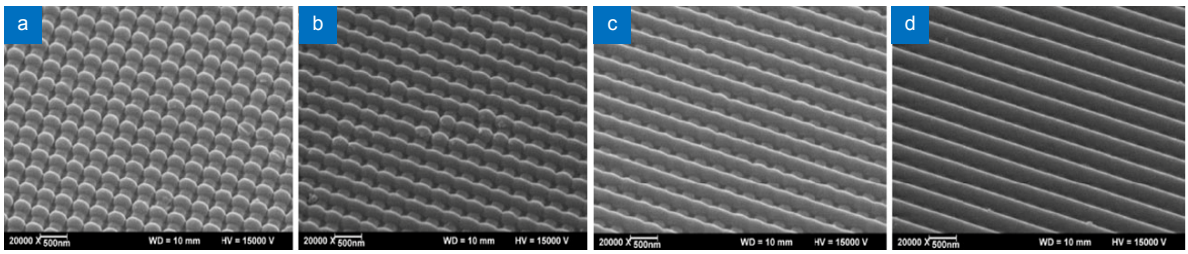

Fig. 16 | SEM images of crossed grating patterns on F2 glass fabricated at 248 nm with the two-grating interferometer with double exposure, 250 mJ/cm2 average fluence. First exposure (generating nearly vertical lines): 200 pulses. The number of pulses of the second exposure (nearly horizontal lines) is increasing from (a) to (d). Figure reprinted with permission from ref.[91], Springer-Verlag Berlin Heidelberg.

research organizations working on such materials. It also promotes the continuous development and breakthrough of laser technology in the field of transparent brittle materials machining. However, there are still some problems in the machining of such materials, such as how to reduce the machining steps, reduce material waste and dry process, and how to continuously improve the overall performance, and make breakthroughs in machining quality, machining efficiency, yield and mass production.

Ultrathin glass substrates and 3D glass are mainly used in the field of flexibility and solar energy. However, such kinds of materials are prone to defects or even cracks during machining. Therefore, how to ensure the mechanical strength requirements after machining will be the challenges for the future applications of this kind of glass.

In recent years, flexible OLEDs and AMOLEDs have developed rapidly. Due to their advantages of lightness, excellent color expression, suitable for full screen, and new side operation dimensions, they will become the next generation mainstream display technology. With the development of this technology, dual 3D glass will be expected to become the most mainstream design scheme of mobile phone in the future, so the machining of dual 3D glass is also a challenging technology.

Many scholars have studied the micro and macro phenomena in the process of LIBWE, such as the pressure of the shock wave, the dynamic characteristics of cavitation bubble, effect of the micro jet and the liquid environment on the etching mechanism. However, the mechanism of LIBWE is not systematic. The stability of laser multifocal stealth dicing system is low, and the adjustment of optical system is difficult. Laser filamentation is a new scientific phenomenon in which complex multi-filament competition brings a challenge for high-precision machining based on the filament effect. Meanwhile, the regular of laser filamentation and its evolution mechanism need further studies. The above complex phenomena and problems need to be solved and further studied.

In short, laser technology plays an important role in the fabrication and applications of micro/nanostructures of transparent brittle materials. With the rapid development of new machining strategies, the fabrication of micro/nano-structures in transparent brittle materials with arbitrary shapes, improved roughness and high resolution may be realized shortly. Undoubtedly, with the support of laser technology, micro/nano-structures and optoelectronic devices based on transparent brittle materials will find increasingly broad applications in both scientific research and practical use in the near future.

References

1. Matsumaru K, Takata A, Ishizaki K. Advanced thin dicing blade for sapphire substrate. *Sci Technol Adv Mater* **6**, 120–122 (2005).
2. Rao R, Bradby J E, Williams J S. Patterning of silicon by indentation and chemical etching. *Appl Phys Lett* **91**, 123113 (2007).
3. Prakash E S, Sadashivappa K, Joseph V, Singaperumal M. Nonconventional cutting of plate glass using hot air jet: experimental studies. *Mechatronics* **11**, 595–615 (2001).
4. Yuan F, Johnson J A, Allred D D, Todd R H. Waterjet cutting of cross-linked glass. *J Vac Sci Technol A* **13**, 136–139 (1995).
5. Clower W, Kaajakari V, Wilson C G. Laser-assisted wet etching of quartz crystal resonators. *J Microelectromechan Syst* **27**, 22–24 (2018).
6. Udrea M V, Alacakir A, Esendemir A, Kusdemir O, Pervan O *et al*. Small-power-pulsed and continuous longitudinal CO_2 laser for material processing. *Proc SPIE* **4068**, 657–662 (2000)
7. Garibotti, Domenick J. Dicing of micro-semiconductors: US3112850. 1963.
8. Yadav A, Kbashi H, Kolpakov S, Gordon N, Zhou K M *et al*. Stealth dicing of sapphire wafers with near infra-red femtosecond pulses. *Appl Phys A* **123**, 369 (2017).
9. Couairon A, Mysyrowicz A. Femtosecond filamentation in transparent media. *Phys Rep* **441**, 47–189 (2007).
10. Banks D P, Kaur K S, Eason R W. Etching and forward transfer of fused silica in solid-phase by femtosecond laser-induced solid etching (LISE). *Appl Surf Sci* **255**, 8343–8351 (2009).
11. Lin G, Tan D Z, Luo F F, Chen D P, Zhao Q Z *et al*. Fabrication and photocatalytic property of α-Bi_2O_3 nanoparticles by femtosecond laser ablation in liquid. *J Alloys Compd* **507**, L43-L46 (2010).
12. Zimmer K, Böhme R, Rauschenbach B. Laser etching of fused silica using an adsorbed toluene layer. *Appl Phys A* **79**, 1883–1885 (2004).
13. Dausinger F, Hugel H, Konov V I. Micromachining with ultrashort laser pulses: from basic understanding to technical applications. *Proc SPIE* **5147**, 106–115 (2003).
14. Foehl C, Breitling D, Jasper K, Radtke J, Dausinger. Precision drilling of metals and ceramics with short- and ultrashort-pulsed solid state lasers. *Proc SPIE* **4426**, 104–107 (2002)
15. Wang Q Y. *Femtosecond Laser Applications in Advanced Technologies* (National Defense Industry Press, Beijing, China 2015).
16. Chichkov B N, Momma C, Nolte S, Von Alvensleben F, Tünnermann A. Femtosecond, picosecond and nanosecond laser ablation of solids. *Appl Phys A* **63**, 109–115 (1996).
17. Ahmed F, Lee M S, Sekita H, Sumiyoshi T, Kamata M. Display glass cutting by femtosecond laser induced single shot periodic void array. *Appl Phys A* **93**, 189–192 (2008).
18. Tsai C H, Liou C S. Fracture mechanism of laser cutting with controlled fracture. *J Manuf Sci Eng* **125**, 519–528 (2003).
19. Ye K D, An C W, Hong M H, Lu Y F. Wafer dicing by laser-induced thermal shock process. *Proc SPIE* **4557**, 442940 (2001).
20. Lan B, Hong M H, Ye K D, Wang Z B, Cheng S X *et al*. Laser precision engineering of glass substrates. *Jpn J Appl Phys* **43**, 7102–7106 (2004).
21. Yamamoto K, Hasaka N, Morita H, Ohmura E. Thermal stress analysis on laser cross scribe of glass. *J Laser Appl* **22**, 937–943 (2010).
22. Hu X B, Hao Q, Guo Z R, Zeng H P. Dicing of sapphire wafer with all-fiber picosecond laser. *Chin J Lasers* **44**, 0102016 (2017).
23. Zhuang H W. Research on multifocal picosecond laser stealth dicing btittle materials (Jiangsu University, Zhenjiang, 2017).
24. Tan B, Venkatakrishnan K. Dual-focus laser micro-machining. *J*

Mod Opt **52**, 2603–2611 (2005).
25. Li Z G. Multi-focal laser processing system: CN103111757A. 2013.
26. Xie H Z, Zhang Y Y, Yang H, Li J, Yi X Y *et al*. Multi-focus femtosecond laser scribing method applied to separation of light emitting diode (LED) device: CN102886609A. 2013.
27. Albermann G, Moeller S, Rohleder T, et al. Plasma etching and stealth dicing laser process: US20160071770, 2016.
28. Lopez J, Mishchik K, Chassagne B, Javaux-Leger C, Hönninger C *et al*. Glass cutting using ultrashort pulsed Bessel beams. In *Proceedings of the International Congress on Applications of Lasers & Electro-Optics Conference* (ResearchGate, 2015);
https://www.researchgate.net/publication/284617626
29. Alexeev A M, Kryzhanovskiy V I, Khait O V. Method for cutting non-metallic materials and device for carrying out said method: EP1506946A2. 2005.
30. Bovatsek J, Arai A Y, Yoshino F. Transparent material processing with an ultrashort pulse laser: US8389891, 2013.
31. Seong C Y, Kim H U, Kim N S, Kim B C. Comparison of laser glass cutting processes using ps and fs lasers. In *International Congress on Applications of Laser & Electro-Optics Conference* (ResearchGate, 2012);
https://www.researchgate.net/publication/292854138.
32. Ji L F, Amina, Yan T Y, Wang W H, Wang T R *et al*. Research progress of ultrafast laser industrial applications based on filamentation. *Opto Electron Eng* **44**, 851–861 (2017).
33. Kovachev L M, Georgieva D A. The long range filament stability: balance between non-paraxial diffraction and third-order nonlinearity. *Proc SPIE* **8770**, 87701G (2013).
34. Daigle J F, Kosareva O, Panov N, Bégin M, Lessard F *et al*. A simple method to significantly increase filaments' length and ionization density. *Appl Phys B* **94**, 249–257 (2009).
35. Braun A, Korn G, Liu X, Du D, Squier J *et al*. Self-channeling of high-peak-power femtosecond laser pulses in air. *Opt Lett* **20**, 73–75 (1995).
36. Brodeur A, Chien C Y, Ilkov F A, Chin S L, Kosareva O G *et al*. Moving focus in the propagation of ultrashort laser pulses in air. *Opt Lett* **22**, 304–306 (1997).
37. Mlejnek M, Wright E M, Moloney J V. Dynamic spatial replenishment of femtosecond pulses propagating in air. *Opt Lett* **23**, 382–384 (1998).
38. Tan D Z, Sharafudeen K N, Yue Y Z, Qiu J R. Femtosecond laser induced phenomena in transparent solid materials: Fundamentals and applications. *Prog Mater Sci* **76**, 154–228 (2016).
39. Song Z M, Zhang Z G, Nakajima T. Transverse-mode dependence of femtosecond filamentation. *Opt Express* **17**, 12217–12229 (2009).
40. Courvoisier F, Zhang J, Bhuyan M K, Jacquot M, Dudley J M. Applications of femtosecond Bessel beams to laser ablation. *Appl Phys A* **112**, 29–34 (2013).
41. Sugioka K, Obata K, Hong M H, Wu D J, Wong L L *et al*. Hybrid laser processing for microfabrication of glass. *Appl Phys A* **77**, 251–257 (2003).
42. Sugioka K, Obata K, Midorikawa K, Hong M H, Wu D J *et al*. Advanced materials processing based on interaction of laser beam and a medium. *J Photochem Photobiol A* **158**, 171–178 (2003).
43. Hong M H, Sugioka K, Lu Y F, Midorikawa K, Chong T C. Laser microfabrication of transparent hard materials and signal diagnostics. *Appl Surf Sci* **186**, 556–561 (2002).
44. Lu X Z, Jiang F, Lei T P, Zhou R, Zhang C T *et al*. Laser-induced-plasma-assisted ablation and metallization on C-plane single crystal sapphire (c-Al_2O_3). *Micromachines* **8**, 300 (2017).
45. Stone A, Sakakura M, Shimotsuma Y, Miura K, Hirao K *et al*. Femtosecond laser-writing of 3D crystal architecture in glass: Growth dynamics and morphological control. *Mater Des* **146**, 228–238 (2018).
46. Pan C F, Chen K Y, Liu B, Ren L, Wang J R *et al*. Fabrication of micro-texture channel on glass by laser-induced plasma-assisted ablation and chemical corrosion for microfluidic devices. *J Mater Process Technol* **240**, 314–323 (2017).
47. Gao H, Hu Y W, Xuan Y, Li J, Yang Y L *et al*. Large-scale nanoshaping of ultrasmooth 3D crystalline metallic structures. *Science* **346**, 1352–1356 (2014).
48. He C, Liu F R, Wang M, Yuan J W, Chen J M. Laser induced backside wet and dry etching of solar glass by short pulse ytterbium fiber laser irradiation. *J Laser Appl* **24**, 022005 (2012).
49. Zelenska K S, Zelensky S E, Poperenko L V, Kanev K, Mizeikis V *et al*. Thermal mechanisms of laser marking in transparent polymers with light-absorbing microparticles. *Opt Laser Technol* **76**, 96–100 (2016).
50. Jiang W, Xie X Z, Wei X, Hu W, Ren Q L *et al*. High contrast patterning on glass substrates by 1064 nm pulsed laser irradiation. *Opt Mater Express* **7**, 1565–1574 (2017).
51. Böhme R, Hirsch D, Zimmer K. Laser etching of transparent materials at a backside surface adsorbed layer. *Appl Surf Sci* **252**, 4763–4767 (2006).
52. Böhme R, Zimmer K. The influence of the laser spot size and the pulse number on laser-induced backside wet etching. *Appl Surf Sci* **247**, 256–261 (2005).
53. Kopitkovas G, Lippert T, Venturini J, David C, Wokaun A. Laser induced backside wet etching: mechanisms and fabrication of micro-optical elements. *J Phys* **59**, 526–532 (2014).
54. Vass C, Hopp B, Smausz T, Ignácz F. Experiments and numerical calculations for the interpretation of the backside wet etching of fused silica. *Thin Solid Films* **453–454**, 121–126 (2004).
55. Zimmer K. Analytical solution of the laser-induced temperature distribution across internal material interfaces. *Int J Heat Mass Transfer* **52**, 497–503 (2009).
56. Zimmer K, Ehrhardt M, Böhme R. Simulation of laser-induced backside wet etching of fused silica with hydrocarbon liquids. *J Appl Phys* **107**, 034908 (2010).
57. Xie X Z, Huang X D, Jiang W, Wei X, Hu W *et al*. Three dimensional material removal model of laser-induced backside wet etching of sapphire substrate with $CuSO_4$ solutions. *Opt Laser Technol* **89**, 59–68 (2017).
58. Huang X D. Numerical simulation and experimental investigation in laser-induced backside wet etching of sapphire (Guangdong University of Technology, Guangzhou, 2015).
59. Sato T, Kurosaki R, Narazaki A, Kawaguchi Y, Niino H. Flexible 3D deep microstructures of silica glass by laser-induced backside wet etching. *Appl Phys A* **101**, 319–323 (2010).
60. Mitsuishi M, Sugita N, Kono I, Warisawa S. Analysis of laser micromachining in silica glass with an absorbent slurry. *CIRP Ann* **57**, 217–222 (2008).
61. Huang Z Q, Hong M H, Do T B M, Lin Q Y. Laser etching of glass substrates by 1064 nm laser irradiation. *Appl Phys A* **93**, 159–163 (2008).
62. Yang Y X, Wang Q X, Keat T S. Dynamic features of a la-

ser-induced cavitation bubble near a solid boundary. *Ultrason Sonochem* **20**, 1098–1103 (2013).
63. Chen Y H, I L. Dynamics of impacting a bubble by another pulsed-laser-induced bubble: jetting, fragmentation, and entanglement. *Phys Rev E* **77**, 026304 (2008).
64. Hu M F. Study on laser induced cavitation bubbles and flow field distribution during laser-induced backside wet etching sapphire substrates (Guangdong University of Technology, Guangzhou, 2014).
65. Xie X Z, Yuan X R, Chen W F, Wei X, Hu W *et al*. New development and applications of laser-induced cavitation bubbles. *Laser Optoelectron Prog* **50**, 080017 (2013).
66. Xie X Z, Hu M F, Chen W F, Wei X, Hu W *et al*. Cavitation bubble dynamics during laser wet etching of transparent sapphire substrates by 1064 nm laser irradiation. *J Laser Micro Nanoeng* **8**, 259–265 (2013).
67. Long J Y, Zhou C X, Cao Z Q, Xie X Z, Hu W. Incubation effect during laser-induced backside wet etching of sapphire using high-repetition-rate near-infrared nanosecond lasers. *Opt Laser Technol* **109**, 61–70 (2019).
68. Lee T, Jang D, Ahn D, Kim D. Effect of liquid environment on laser-induced backside wet etching of fused silica. *J Appl Phys* **107**, 033112 (2010).
69. Liu X M, Long Z, He J, Liu X H, Hou Y F *et al*. Temperature effect on the impact of a liquid-jet against a rigid boundary. *Optik* **124**, 1542–1546 (2013).
70. Soliman W, Nakano T, Takada N, Sasaki K. Modification of Rayleigh-Plesset theory for reproducing dynamics of cavitation bubbles in liquid-phase laser ablation. *Jpn J Appl Phys* **49**, 116202 (2010).
71. Cao Z Q, Xie X Z, Chen W F, Wei X, Hu W *et al*. Research progress of pressure detection and applications in liquid-assisted laser machining. *Opto-Electron Eng* **44**, 381–392 (2017).
72. Cao Z Q. Study on the detection of cavitation and pressure in the process of laser induced backside wet etching of sapphire substrates. (Guangdong University of Technology, Guangzhou, 2018).
73. Qiao L L, He F, Wang C, Cheng Y, Sugioka K *et al*. A microfluidic chip integrated with a microoptical lens fabricated by femtosecond laser micromachining. *Appl Phys A* **102**, 179–183 (2011).
74. Liu J, Zhang Z, Lu Z, Xiao G, Sun F *et al*. Fabrication and stitching of embedded multi-layer micro-gratings in fused silica glass by fs laser pulses. *Appl Phys B* **86**, 151–154 (2007).
75. Queste S, Salut R, Clatot S, Rauch J Y, Khan Malek C G. Manufacture of microfluidic glass chips by deep plasma etching, femtosecond laser ablation, and anodic bonding. *Microsyst Technol* **16**, 1485–1493 (2010).
76. Ji L F, Hu Y, Li J, Wang W H, Jiang Y J. High-precision micro-through-hole array in quartz glass machined by infrared picosecond laser. *Appl Phys A* **121**, 1163–1169 (2015).
77. Gao X Y. Study on the development of working solution and processing mechanism of laser wet etching sapphire Substrat (Guangdong University of Technology, Guangzhou, 2014).
78. Jiang W. Study on the mechanism of micro Nano suspended particle assisted laser-induced backside wet dicing of sapphire substrate. (Guangdong University of Technology, Guangzhou, 2017).
79. Shen J J, Luo G X, Pan Y, Liu Z J, Jiang Z H. Research on glass cutting process base on 532 nm wavelength nanosecond laser. *Appl Laser* **35**, 493–499 (2015).
80. Rolo A, Coelho J, Pires M. Laser glass marking: influence of pulse characteristics. *Proc SPIE* **5958**, 59583D (2005).
81. Nakazumi T, Sato T, Narazaki A, Niino H. Laser marking on soda-lime glass by laser-induced backside wet etching with two-beam interference. *J Micromechan Microeng* **26**, 095015 (2016).
82. Dumont T, Lippert T, Wokaun A, Leyvraz P. Laser writing of 2D data matrices in glass. *Thin Solid Films* **453–454**, 42–45 (2004).
83. Zhang X M, Ma J Q, Ding Y F. Analysis of marking glass with different process parameters based on super-pulsed laser. *Adv Mater Res* **602–604**, 929–933 (2013).
84. Sato T, Narazaki A, Niino H. Fabrication of micropits by LIBWE for laser marking of glass materials. *J Laser Micro/Nanoeng* **12**, 248–253 (2017).
85. Ding X, Yasui Y, Kawaguchi Y, Niino H, Yabe A. Laser-induced back-side wet etching of fused silica with an aqueous solution containing organic molecules. *Appl Phys A* **75**, 437–440 (2002).
86. Ding X, Kawaguchi Y, Niino H, Yabe A. Laser-induced high-quality etching of fused silica using a novel aqueous medium. *Appl Phys A* **75**, 641–645 (2002).
87. Ding X M, Sato T, Kawaguchi Y, Niino H. Laser-induced backside wet etching of sapphire. *Jpn J Appl Phys* **42**, 176–178 (2003).
88. Wang J, Niino H, Yabe A. Micromachining of quartz crystal with excimer lasers by laser-induced backside wet etching. *Appl Phys A* **69**, S271–S273 (1999).
89. Niino H, Kawaguchi Y, Sato T, Narazaki A, Gumpenberger T *et al*. Laser ablation of toluene liquid for surface micro-structuring of silica glass. *Appl Surf Sci* **252**, 4387–4391 (2006).
90. Sohn I B, Choi H K, Yoo D, Noh Y C, Sung J H *et al*. Synchronized femtosecond laser pulse switching system based nano-patterning technology. *Opt Mater* **69**, 295–302 (2017).
91. Bekesi J, Meinertz J, Simon P, Ihlemann J. Sub-500-nm patterning of glass by nanosecond KrF excimer laser ablation. *Appl Phys A* **110**, 17–21 (2013).

Acknowledgements

This work is partially supported by the National Natural Science Foundation of China (51575114 and 51805093), the National Key R&D Program of China (2018YFB1107700) and Guangzhou Science and Technology Project (201607010156).

Competing interests

The authors declare no competing financial interests.